Stress analysis of a gravity dam by the finite element method

R. W. CLOUGH (1) AND E. L. WILSON (2)

RÉSUMÉ

Des études préalables ont montré que la méthode de l'élément fini est un instrument très adapté à l'analyse des états plans de contrainte. Dans la présente communication on décrit l'application de cette méthode à l'analyse de contraintes dans un barrage poids. On a généralisé le programme de la calculatrice digitale de façon à pouvoir tenir compte automatiquement des contraintes thermiques, de celles dues aux poids propre ainsi que des surcharges arbitraires et aussi de façon à pouvoir faire l'analyse par un procédé d'itération. On présente les résultats obtenus pour différentes hypothèses de chargement afin de montrer l'efficacité de la méthode.

SUMMARY

In previous studies, the finite element method has been shown to provide a convenient tool for the analysis of plane stress systems. The present paper is concerned with the application of this method to stress analysis of a gravity dam. The digital computer program has been extended to account automatically for thermal and dead weight stresses as well as arbitrary live loads, and makes use of an iteration procedure in performing the analysis. Results are described for a number of different loading conditions to demonstrate the effectiveness of the procedure.

INTRODUCTION

The matrix algebra formulation of the equations of structural analysis completely generalizes the analytical procedures, and greatly broadens the scope of their applicability. Traditionally, use of the standard methods of structural analysis has been restricted to the treatment of structures built up from one-dimensional members, i.e. members whose elastic and geometric properties can be expressed as functions of position along the elastic axis. Through the use of matrix procedures, however, the same basic principles can be applied in the analysis of entirely different types of structures-comprising assemblages of two-dimensional elements. Included among such structures might be plates, shells, and systems subjected to plane stress or plane strain.

The purpose of this paper is to describe the application of matrix structural analysis methods to the solution of a plane stress elasticity problem. The

(1) Professor of Civil Engineering, University of California, Berkeley, California, U.S.A.

(2) Graduate student, University of California, Berkeley, California, U.S.A.

general procedure, which is known as the finite element method, has been described in a previous publication[1]. However, although the versatility and range of accuracy of the method were indicated in that report, its usefulness in solving large-scale, practical problems had not yet been demonstrated. For this reason, the authors were pleased to be given the opportunity of undertaking the investigation described in this report: the application of the finite element method to the analysis of stresses and displacements in a large concrete gravity dam. The investigation was sponsored by the Little Rock District Office of the U. S. Army Corps of Engineers, and a complete report: on the studies has been submitted to that office[2]. Due to space limitations, only a brief summary of the work and a representative selection from the final results will be presented here.

STATEMENT OF THE PROBLEM

The system considered in this investigation was a one foot thick slice of a concrete gravity dam, 196 feet high from the base to the spillway crest, with a profile as shown in figure 1. Of particular interest in the study was the effect on the stress distribution of a crack extending from the foundation rock vertically through most of the height of the section, as shown in the sketch. The loadings to which the structure was sujected included the weight of the concrete, the water pressures, and thermal loads caused by temperature changes (Fig. 2).

Properties assumed for the concrete and for the foundation rock in these analyses are shown in Table I. It will be noted that different moduli of elasticity were assumed for the two materials; the relatively low modulus taken for the concrete was intended to account for the effects of creep and plastic flow under sustained load. In one phase of the study, an orthotropic elasticity condition was assumed in the foundation rock (with the vertical modulus only one-fifth of the horizontal) because it is quite possible that horizontal stratification of the foundation might produce such a condition, and it was of interest to determine the resulting effect on the stress distribution in the dam.

TABLE I. Assumed properties of materials

Concrete:		
Modulus of Elasticity	E_c	$= 2.0 \times 10^6$ psi
Poisson's Ratio	υ	$= 0.17$
Unit Weight	γ_c	$= 150$ pcf
Thermal Coefficient	α	$= 7.0 \times 10^{-6}$ per °F
Foundation Rock:		
Modulus of Elasticity	E_f	$= 5.0 \times 10^6$ psi
Poissons' Ratio	υ	$= 0.17$
Thermal Coefficient	α	$= 7.0 \times 10^{-6}$ per °F
Vertical Modulus (Orthotropic cases)	E_{fy}	$= 1.0 \times 10^6$ psi
Water:		
Unit Weight	γ_w	$= 62.5$ pcf

Temperature Change:

$\Delta T = -35°$ F in body of dam decreasing to 0° F about 30 feet below the surface of the foundation rock (Fig. 2).

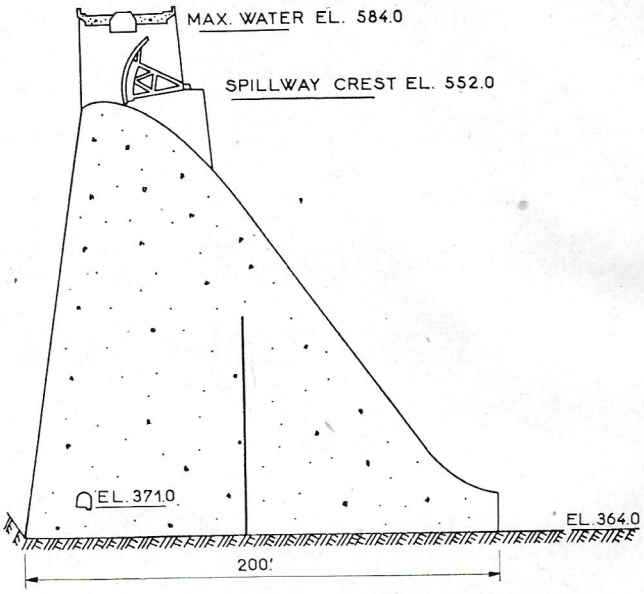

FIG. 1. — **Basic geometry of the dam section.**

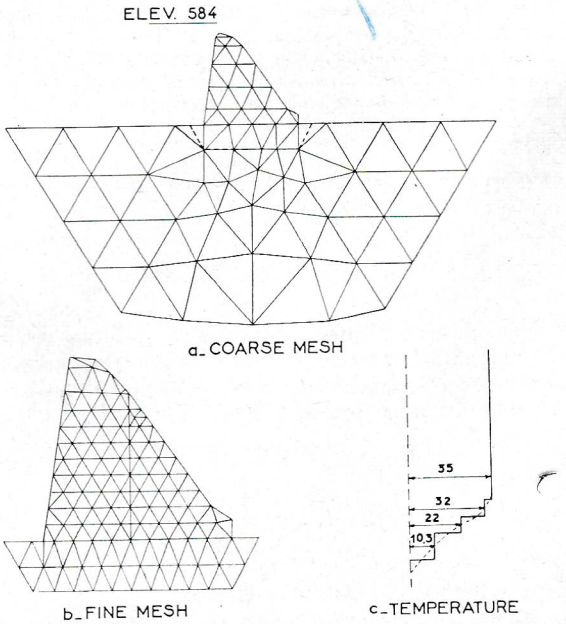

FIG. 2. — **Finite element idealizations of the dam section.**

It was assumed in these studies that the vertical crack resulted from the cooling of the concrete, and the evaluation of the width of the crack opening resulting from each of the various load combinations was one of the principal objects of the studies. In addition, the stress distribution within the section (particularly in the stress concentration zones at the ends of the crack and at the toe and heel of the dam) as well as its overall displacements were of interest. An uncracked section also was studied so that a comparison of the results for the two systems might demonstrate directly the influence of the crack.

THE FINITE ELEMENT METHOD

Because the finite element method has been described previously, only a brief description of the general features of the method will be given here. In addition, certain features of the present study which have not been presented before will be discussed in greater detail. In general, the method consists of idealizing the actual continuous system as an assemblage of triangular plate elements, interconnected only at the corners, and also loaded only at these points. Within each element, the normal and shear stresses are assumed uniform, thus continuity between the elements is maintained even though they are connected only at the nodal points.

The analysis involves first calculating the stiffnesses of the individual triangular elements; then by adding together the pertinent element stiffnesses, the stiffness of the assembled system is determined. This assembled structure stiffness is represented by the matrix [K] in the equation:

$$\{R\} = [K]\{r\} \tag{1}$$

where also

$\{R\}$ = vector of all nodal point force components
$\{r\}$ = vector of corresponding nodal point displacements.

This equation can be solved formally for the displacements resulting from specified loads by inverting the stiffness matrix. However, in the present study, this matrix was too large to be inverted conveniently, and the displacements were determined from Eq. (1) by an iteration process.

After the nodal point displacements have been obtained, the stress components in each of the triangular elements (which are linearly related to the displacements) can be obtained by the matrix multiplication:

$$\{\sigma\} = [M]\{r\} \tag{2}$$

in which

$\{\sigma\}$ = vector of all element stresses σ_x, σ_y, τ_{xy}
$[M]$ = stress transformation matrix.

In this study, the principal stresses in the elements and their directions were also determined, in addition to the x, y stresses.

Element Idealizations

The finite element idealizations used in this study are shown in figure 2. The coarse mesh idealization in figure 2*a* was used in preliminary analyses in order to determine the displacements at the base of the foundation system used in the fine mesh analysis (shown by the dashed line). Thus it was possible to retain the effect of a deep foundation in the fine mesh idealization shown in figure 2*b* without devoting a large number of elements to the foundation zone. It was necessary, of course, to make a separate coarse mesh analysis for each of the loading conditions which were applied to the fine mesh system. In the coarse mesh system, there are a total of 103 elements and 69 nodal points, while in the fine mesh system the numbers are 194 and 130 respectively.

Element Stiffness

The derivation of the stiffness matrix of an arbitrary isotropic plane stress element is presented in [1], and will not be repeated here. It is of interest to note, however, that this same stiffness matrix can be applied in a plane strain analysis if modified material properties are used, as follows:

$$E^* = \frac{E}{1-\nu^2}$$
$$\nu^* = \frac{\nu}{1-\nu} \tag{3}$$

where E = modulus of elasticity (actual)
ν = Poissons' ratio (actual)

and the starred values represent the modified properties to be used in a plane strain analysis. The plane stress condition was considered to be more applicable in the present study; but with the assumed value of Poisson's ratio, the difference between the two conditions is negligible: $E^*/E = 1.03$, $\nu^*/\nu = 1.20$.

In order to represent the orthotropic foundation material, it was necessary to develop an orthotropic element stiffness matrix. For this purpose, the stress-strain relationship for an orthotropic material was needed. In this derivation, it was assumed that the orthotropic material actually consisted of a horizontally layered system of alternately hard and soft isotropic materials. Designating the properties of these materials E_1, ν_1 and E_2, ν_2 respectively, it was further assumed that:

$$\frac{E_1}{\nu_1} = \frac{E_2}{\nu_2} \tag{4}$$

On the basis of these assumptions, the orthotropic stress-strain relationship was found to be

$$\begin{bmatrix} \varepsilon_x \\ \varepsilon_y \\ \gamma_{xy} \end{bmatrix} = \frac{1}{E_x} \begin{bmatrix} 1 & -\nu_x & 0 \\ -\nu_x & \mu & 0 \\ 0 & 0 & 2(\mu + \nu_x) \end{bmatrix} \tag{5}$$

in which

$$E_x = E_1 (1 - r^*); \; r^* = r\left(1 - \frac{E_2}{E_1}\right)$$

$$\nu_x = \nu_1 \; (1 - r^*)$$

$$\mu = \frac{E_x}{E_y}; \; E_y = \frac{E_2}{r^* + \frac{E_2}{E_1}}$$

and r is the proportion of the total volume occupied by the soft layers. Using this orthotropic stress-strain law, the derivation of the orthotropic element stiffness followed exactly the procedure described in [1] for the isotropic triangular element stiffness.

Loadings

The load vector $\{R\}$ in Eq. (1) is merely a listing of all the load components applied at the nodal points in any given analysis. For each nodal point, the dead load force was computed by taking one-third of the total weight of all elements attached to the nodal point. Live load (water) forces were applied only at the nodal points in contact with the water, of course, and were taken as the concentrated static equivalent of the distributed water pressures acting on these elements.

The thermal loads were calculated by first determining the stresses which would exist if all strains due to temperature changes were constrained. In a plane stress system, these stresses are given by

$$\sigma = -\frac{E\alpha}{1 - \nu} \Delta T \qquad (6)$$

in which α = thermal coefficient of expansion
ΔT = change of temperature.

The nodal forces required to maintain these stresses in each element were then found by simple statics. Finally, since these nodal constraints did not really exist, their effect was eliminated by applying equal and opposite nodal forces.

These *reversed* nodal forces are the thermal loads for which the section was analyzed. Displacements resulting from these effective loads are the true thermal displacements in the system. The total thermal stresses were determined by combining the constrained stress of Eq. (6) with the stresses resulting from these thermal loads.

THE DIGITAL COMPUTER PROGRAM

Practical applications of the finite element method described above require such a tremendous amount of computational effort that they may be performed only by means of automatic digital computers. A special program designed to perform such analyses for arbitrary finite element idealizations has been written for the IBM 704 operated by the University of California Computer Center, and was used in all of the work described in this report.

The computer program performs three major tasks in the complete analysis of a plane stress system. First, the element stiffness and load matrices are formed from a basic numerical description of the structure. Second, Eq. (1) is solved for the displacements of the nodal points by an iteration procedure. Third, the internal element stresses are determined from these displacements. Only the main operations of the computer program will be described here; details of the coding will be omitted. The operation of the program is flexible in that both input and output can be « on-line » or may be effected « off-line » through the use of magnetic tapes and peripheral equipment.

Numerical Procedure

Before presenting the sequence of operations that is performed by the computer program, it is necessary to discuss in some detail the actual numerical procedure that was employed. This method is a modification of the well-known Gauss-Seidel iteration procedure which, when applied to Eq. (1), involves the repeated calculation of new displacements from the equation

$$r_n^{(s+1)} = (k_{nn})^{-1} \left[R_n - \sum_{i=1,n-1} k_{ni} r_i^{(s+1)} - \sum_{i=n+1,N} k_{ni} r_i^{(s)}\right] \qquad (7)$$

where n = number of the displacement component
s = cycle of iteration

The only modification of the procedure introduced in this analysis is the application of Eq. (7) simultaneously to both components of the displacement at each nodal point. Therefore r_n and R_n become vectors with x and y components, and the stiffness coefficients are in the form

$$k_{lm} = \begin{bmatrix} k_{xx} & k_{xy} \\ k_{yx} & k_{yy} \end{bmatrix}_{lm} \qquad (8)$$

in which l and m are nodal point numbers.

Over-Relaxation Factor

The rate of convergence of the Gauss-Seidel procedure can be greatly increased by the use of an over-relaxation factor [3]. However, in order to apply this factor it is first necessary to calculate the change in the displacement of nodal point n between cycles of iteration:

$$\Delta r_n^{(s)} = r_n^{(s+1)} - r_n^{(s)}. \qquad (9)$$

The substitution of Eq. (7) into Eq. (9) yields for the change in displacement

$$\Delta r_n^{(s)} = (k_{nn})^{-1} \left[R_n - \sum_{i=1,n-1} k_{ni} r_i^{(s+1)} - \sum_{i=n,N} k_{ni} r_i^{(s)}\right] \qquad (10)$$

The new displacement of nodal point n is then determined from the following equation:

$$r^{(s+1)} = r_{nn}^{(s)} + \beta \Delta r_n^{(s)} \qquad (11)$$

where β is the over-relaxation factor. For the structure considered in this report it was found that a value of β equal to 1.86 gave the most rapid convergence.

Physical Interpretation of Method

Important physical significance can be attached to the terms of Eq. (10). The term $(k_{nn})^{-1}$ is the flexibility of nodal point n. This represents the nodal point displacements resulting from unit nodal point forces, and can be written in the form of a sub-matrix:

$$(k_{nn})^{-1} = \begin{bmatrix} f_{xx} & f_{xy} \\ f_{yx} & f_{yy} \end{bmatrix}_n . \qquad (12)$$

The summation terms represent the elastic forces acting at nodal point n due to the deformations of the plate elements:

$$Q_n^{(s+1)} = \sum_{i=1,n-1} k_{ni} r_i^{(s+1)} + \sum_{i=n,N} k_{ni} r_i^{(s)} . \qquad (13)$$

The difference between these elastic forces and the applied loads is the total unbalanced force, which in sub-matrix form may be written:

$$\begin{Bmatrix} X \\ Y \end{Bmatrix}_n^{(s+1)} = \begin{Bmatrix} R_x \\ R_y \end{Bmatrix}_n - \begin{Bmatrix} Q_x \\ Q_y \end{Bmatrix}_n^{(s+1)} . \qquad (14)$$

Equation (11) which gives the new displacement of nodal point n, may now be written in the following sub-matrix form:

$$\begin{Bmatrix} r_x \\ r_y \end{Bmatrix}_n^{(s+1)} = \begin{Bmatrix} r_x \\ r_y \end{Bmatrix}_n^{(s)} + \beta \begin{bmatrix} f_{xx} & f_{xy} \\ f_{yx} & f_{yy} \end{bmatrix}_n \begin{Bmatrix} X \\ Y \end{Bmatrix}_n^{(s+1)} . \qquad (15)$$

It is important to note that any desired nodal point displacement may be assumed for the first cycle of iteration. A good choice of these displacements will greatly speed the convergence of the solution. In fact, if all displacements were assumed correctly, the unbalanced forces given by Eq. (14) would be zero, and no iteration would be necessary. However, in a practical case, there always will be unbalanced forces in the system at first, and the iteration process continually reduces them toward zero.

Input Data

For the purpose of defining the structure, all nodal points and elements are numbered, consecutively. The numerical description is read into the machine in the form of punched cards, by the following four arrays:

A. Parameter Array (6 numbers):
1. Number of elements.
2. Number of nodal points.
3. Number of boundary points.
4. Over-relaxation factor β.
5. Convergence limit.
6. Coefficient of thermal expansion α.

B. Element Array (9 numbers per element):
1. Element number.
2. Number of nodal point i.
3. Number of nodal point j.
4. Number of nodal point k.
5. Modulus of elasticity E
6. Poisson's ratio υ
7. Unit weight of element γ
8. Temperature change within element ΔT
9. Orthotropic factor $\mu = \frac{E_x}{E_y}$

C. Nodal Point Array (7 numbers per nodal point):
1. Nodal point number.
2. x-ordinate.
3. y-ordinate,
4. x-load.
5. y-load.
6. Initial x-displacement.
7. Initial y-displacement.

D. Boundary Condition (2 numbers per boundary point):
1. Nodal point number.
2. This number indicates the type of constraint: « O » for a point fixed both vertically and horizontally, the only boundary constraint condition considered in this investigation.

Output Information

At specified intervals in the iteration procedure, nodal displacements and element stresses are printed. Figure 3 illustrates the form of the computer output in a typical case. In addition, the sum of the absolute magnitude of the unbalanced forces at all nodal points (Eq. 14), which is computed for each cycle, is printed out as a check on the convergence of the procedure. In all analyses made during the course of this investigation, this sum was reduced to less than 1/1000 of its value after the first cycle of iteration.

Timing

The computational time required by the program is approximately equal to 0.07 n.m seconds, where n equals the number of nodal points and m equals the number of cycles of iteration. The number of cycles required depends on the accuracy of the initially assumed displacements and on the desired degree of convergence. For the structure considered in this report, the computer time per solution was approximately 7 minutes for the coarse mesh and 17 minutes for the fine mesh. The number of cycles of iteration for the various cases ranged from about 70 to 100.

RESULTS

Although the printed output of the computer, as shown in figure 3, contained the complete results of the investigation, they were also presented graphi-

ELEMENT	(PSI) X-STRESS	(PSI) Y-STRESS	(PSI) XY-STRESS	(PSI) MAX-STRESS	(PSI) MIN-STRESS	(DEGREES) DIRECTION
1	-21.637024	-40.614304	33.432649	3.6	-65.9	-37.1
2	15.095711	3.577621	21.158474	31.3	-12.6	-37.4
3	-42.514305	-38.270859	2.591661	-37.0	-43.7	-64.7
4	-31.742538	-16.989304	14.911327	-7.7	-41.0	-58.2
5	-5.087471	9.535896	-4.226090	10.7	-6.2	75.0
6	-60.592682	-21.883614	5.673300	-21.1	-61.4	-81.8
7	3.596840	-6.501434	8.060141	8.1	-11.0	-29.0
8	-41.907402	8.325272	22.115488	16.7	-50.3	-69.3
9	-29.894760	-14.201363	2.760811	-13.7	-30.4	-80.3
10	-19.019836	-113.042328	41.108610	-3.6	-128.5	-20.6
11	-9.670067	-3.545715	1.172920	-3.3	-9.9	-79.5
12	-19.362946	24.689590	0.280712	24.7	-19.4	-89.6
13	-42.158066	2.489532	-3.621626	2.8	-42.4	85.4
14	-13.876846	9.762047	-1.376879	9.8	-14.0	86.7
15	-55.332329	12.838753	11.194128	14.6	-57.1	-80.9
16	-11.221085	21.112564	13.384552	25.9	-16.0	-70.2
17	-61.941177	-16.112938	31.179846	-0.3	-77.7	-63.2
18	14.900993	-10.251991	33.216614	37.8	-33.2	-34.6
19	-77.299423	-18.673866	45.481194	6.1	-102.1	-61.4
20	-68.392212	-25.644630	21.986590	-16.4	-77.7	-67.1
21	-34.477783	-10.517090	11.790384	-5.7	-39.3	-67.7
22	-7.344345	8.977432	-4.832099	10.3	-8.7	74.7
23	-34.220215	23.321732	-8.167995	24.5	-35.4	82.1
24	-11.582161	32.631912	-2.718958	32.8	-11.7	86.5
25	-46.657974	19.291512	3.835845	19.5	-46.9	-86.7
26	-13.946526	43.675842	18.032915	48.9	-19.1	-74.0
27	-83.458755	-12.719467	45.440448	9.5	-105.7	-63.9
28	-4.890427	13.208176	37.164865	42.4	-34.1	-51.8
29	1.348351	-10.524033	30.664423	26.6	-35.8	-39.5
30	-102.706940	-89.829132	46.319461	-49.5	-143.0	-49.0
31	-36.349174	-70.508469	66.600939	15.3	-122.2	-37.8
32	-1.370247	-44.906326	25.714500	10.6	-56.8	-24.9
33	-26.064774	-64.952545	59.050345	16.7	-107.7	-35.9
34	-20.962494	-16.453156	14.811054	-3.7	-33.7	-49.3
35	-32.728851	-5.217323	2.676623	-5.0	-33.0	-84.5
36	-45.844315	15.385841	-0.936499	15.4	-45.9	89.1
37	-22.696800	12.184837	-2.723261	12.4	-22.9	85.6
38	-9.309067	33.630989	-7.344516	34.9	-10.5	80.6
39	-16.388954	38.171394	-4.737985	38.6	-16.8	85.1
40	29.606812	46.513466	2.932751	47.0	29.1	-80.4
41	-6.309235	29.010864	-7.292584	30.5	-7.8	78.8
42	41.728279	65.571236	81.198050	135.7	-28.4	-49.2
43	-18.289627	-15.782555	19.939212	2.9	-37.0	-46.8
44	22.005043	-23.887611	62.266115	65.4	-67.3	-34.9
45	-9.252480	-55.976212	39.016029	12.9	-78.1	-29.5
46	-23.453789	-69.528412	51.371544	9.8	-102.8	-32.9
47	-57.654015	-19.821014	12.165121	-16.2	-61.2	-73.6
48	-16.010735	-1.447845	13.872331	6.9	-24.4	-58.8
49	-53.434456	6.212318	3.402412	6.4	-53.6	-86.7
50	-11.542534	29.182938	16.814773	35.2	-17.6	-70.2
51	-33.487152	19.204918	16.218376	23.8	-38.1	-74.2

NODAL POINT	(INCHES) X-DISPLACEMENT	(INCHES) Y-DISPLACEMENT
1	0.045173	-0.029458
2	0.058178	-0.013816
3	0.130151	-0.034537
4	0.166736	-0.067413
5	0.190258	-0.100647
6	0.209396	-0.136003
7	0.225354	-0.171480
8	0.238976	-0.207627
9	0.250559	-0.243729
10	0.261115	-0.279447
11	0.272950	-0.320961
12	0.289812	-0.371849
13	0.297384	-0.398693
14	0.238857	-0.416963
15	0.237644	-0.395673
16	0.191532	-0.400589
17	0.232356	-0.337109
18	0.190137	-0.351804
19	0.149180	-0.364911
20	0.141777	-0.380089
21	0.129665	-0.372276
22	0.238763	-0.288985
23	0.196613	-0.306839
24	0.154202	-0.323265
25	0.111614	-0.336806
26	0.087621	-0.344180
27	0.201616	-0.264921
28	0.159523	-0.282565
29	0.117430	-0.297379
30	0.096284	-0.302664
31	0.090143	-0.324456
32	0.068399	-0.327413
33	0.070444	-0.305661
34	0.046395	-0.305916
35	0.205631	-0.222702
36	0.163587	-0.241099
37	0.123230	-0.257917
38	0.084663	-0.269945
39	0.071567	-0.268477
40	0.048155	-0.267604
41	0.016155	-0.265461
42	0.207651	-0.180322
43	0.164601	-0.199870
44	0.122949	-0.217015
45	0.083207	-0.233610

FIG. 3. — **Digital computer output.**

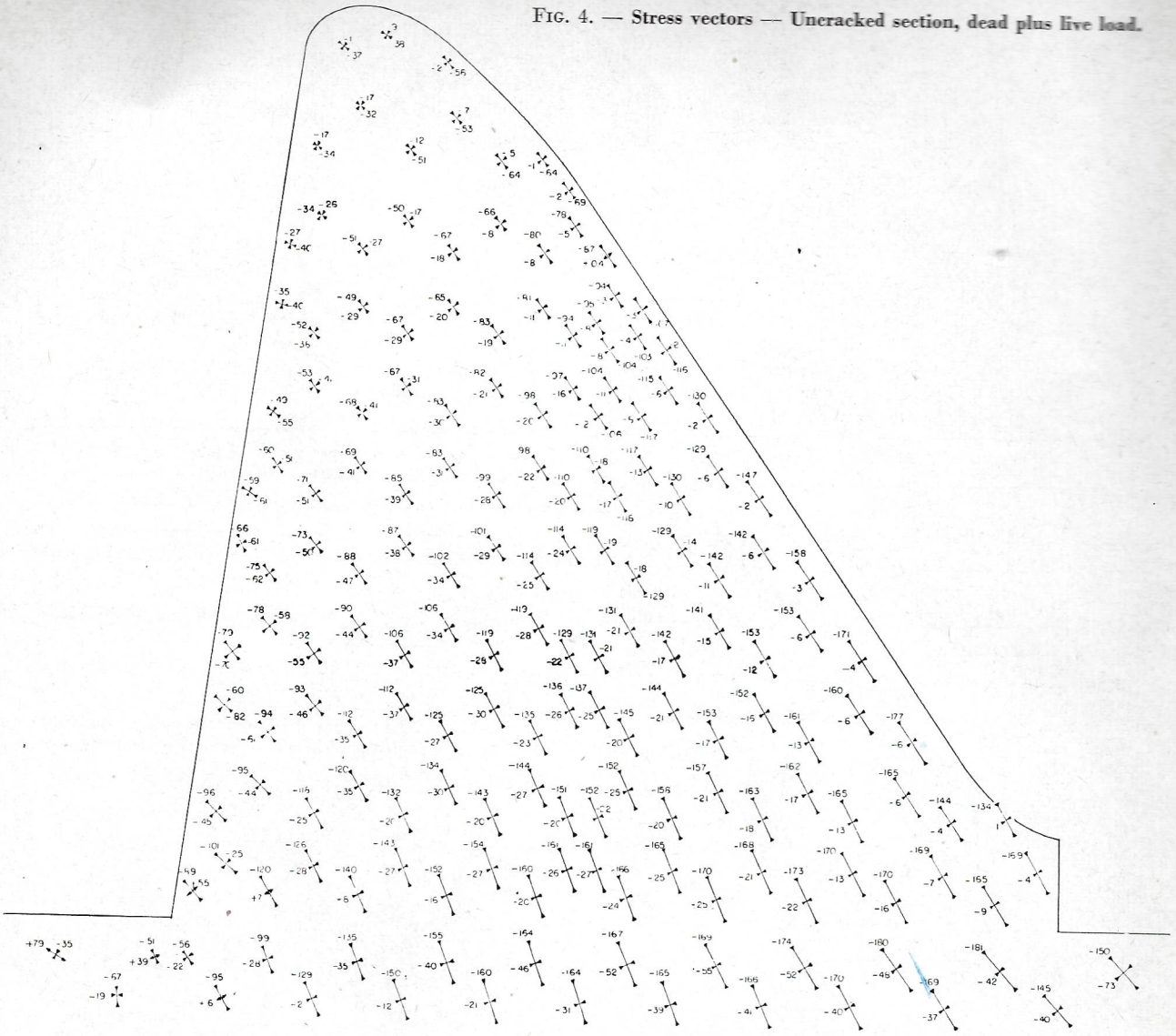

FIG. 4. — **Stress vectors — Uncracked section, dead plus live load.**

cally in order that they might be more easily interpreted. Stress results were presented in two types of charts. Stress Vectors, shown in figure 4 for the dead plus live load acting on the uncracked section, are merely a direct graphical representation of the magnitudes and directions of the principal stresses, plotted from the center of each element. Such figures give a good qualitative picture of the state of stress in the section; but for quantitative studies, the Stress Contours, shown in figures 5, 6, and 7 are preferable. These contours, or iso-static lines, are lines of constant stress on the section. They clearly indicate the areas of high stress concentration.

Although it is not the purpose of this paper to discuss the specific results obtained in the investigation, a few comments with regard to these figures may be of interest. Figure 5 shows the stress distribution in the section with a crack extending through 7/9 of the height, when subjected to dead plus live loads. The compressive stress concentrations at the base and top of the crack, and the tensile stress zones at the heel and near the top of the crack are of particular interest here. A comparison of the two cases shown in figure 6 demonstrates the importance of the temperature stresses on the uncracked section, in comparison with those due to dead plus live loading. Comparison of figure 7 with figure 5*a* indicates the relatively small influence exerted by the reduced vertical modulus of the orthotropic foundation.

Nodal displacement results were also presented in two types of charts. Figure 8 shows the boundary nodal point displacement vectors. Lines connecting the ends of these vectors show the outline of the deformed structure, to an exaggerated scale. Of more interest in this investigation, however, was the

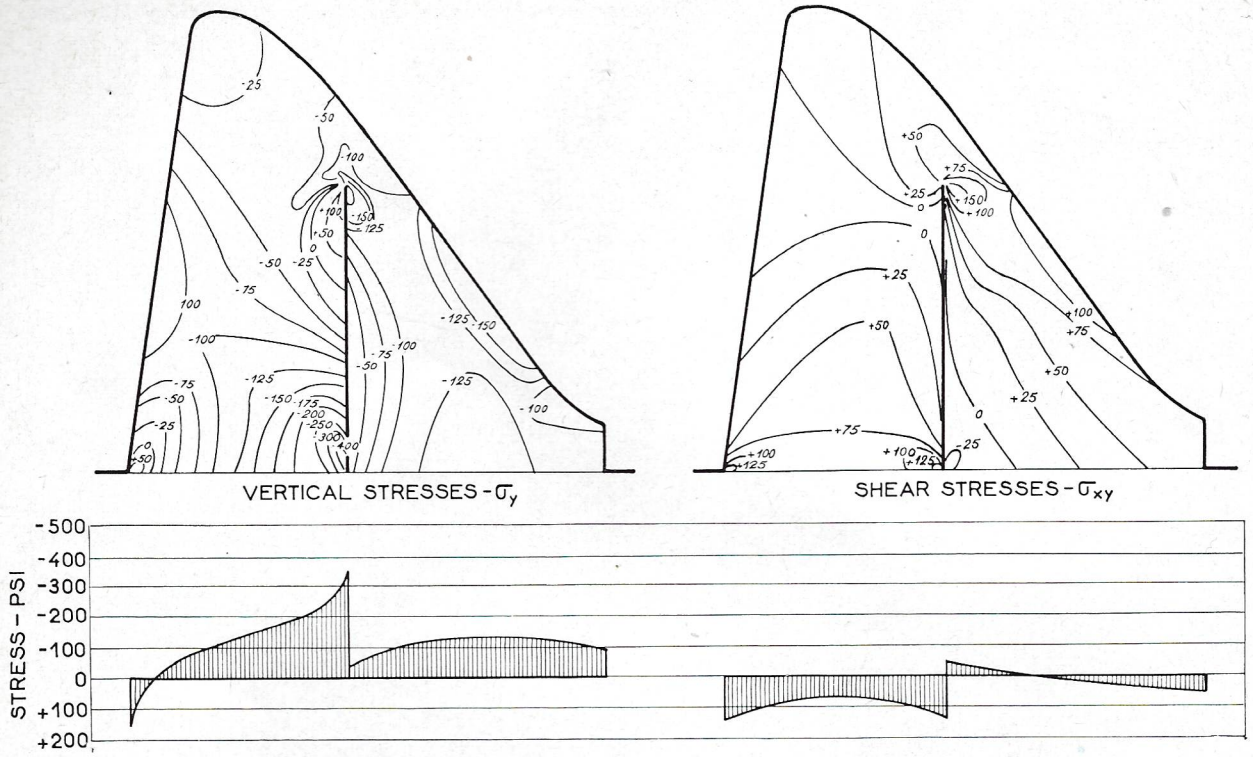

FIG. 5. — **Stress contours — 7/9 crack height, dead plus live load.**

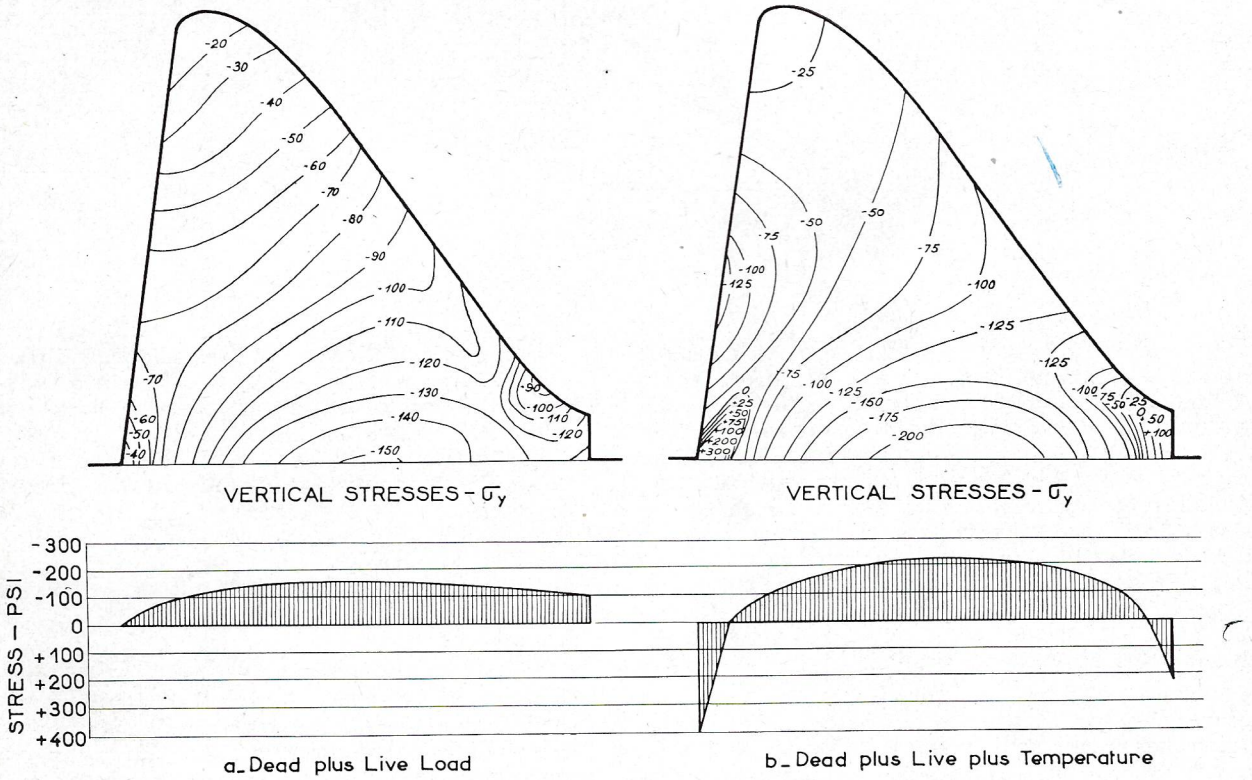

FIG. 6. — **Influence of temperature on normal stress distribution — uncracked section.**

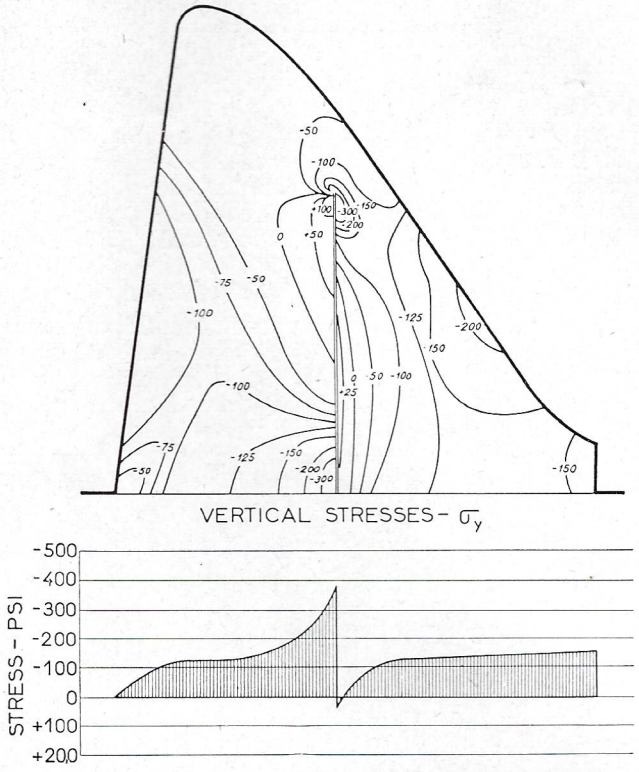

FIG. 7. — **Normal stress distribution with orthotropic foundation — 7/9 crack height— dead plus live load.**

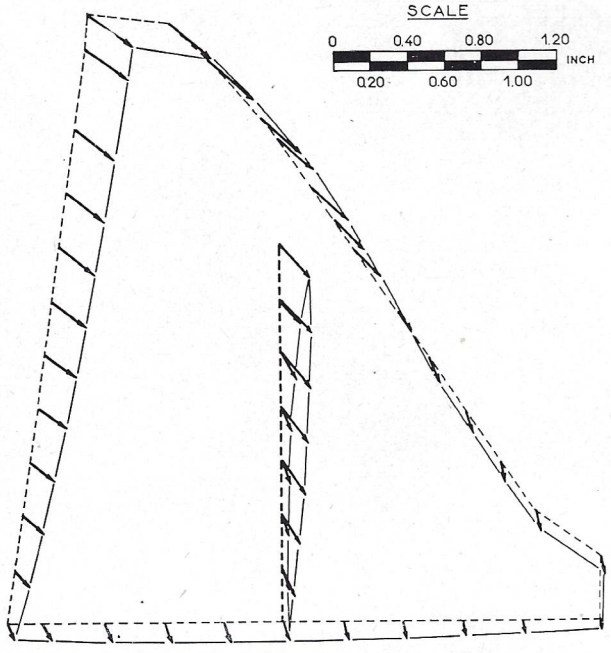

FIG. 8. — **Boundary displacements — 7/9 crack height, dead plus live load.**

relative displacement of the two sides of the crack, shown in figure 9. Here the successive effects of temperature, dead load, and dead plus live load on the crack opening are clearly indicated. It is of interest to note that the live loading was not sufficient to close the crack completely.

CONCLUSIONS

This investigation has clearly demonstrated the applicability and practicality of the finite element method in solving large-scale and complex plane stress (or plane strain) elasticity problems. One of the most important attributes of the method is its versatility, which results from its discrete (rather than continuous) representation of the system. Because each element is treated individually, it may be assigned properties completely without regard for the properties of its neighbours. Thus, the diffe-

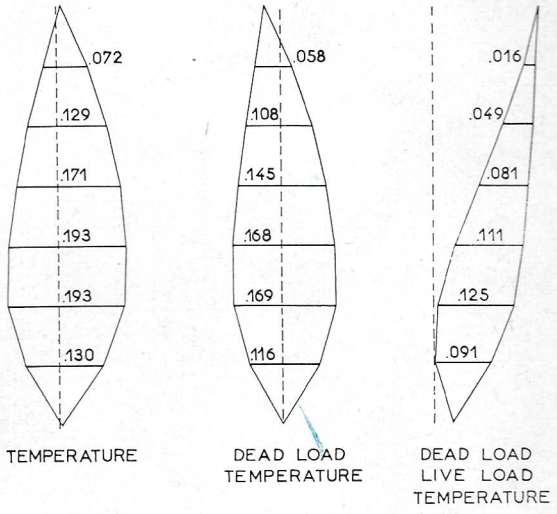

FIG. 9. — **Crack openings — 7/9 crack height.**

rence between the moduli of the foundation rock and the concrete of the dam, and the fact that one material might be orthotropic while the other was isotropic, caused no difficulty whatsoever. Similarly, because the temperature changes were assigned element by element, any desired thermal gradient could be represented.

Also to be noted is the ease with which the triangular element system can be arranged to fit any specified boundary condition. The internal crack becomes merely another external boundary by this procedure, and leads to no special problems. Another advantage of the triangular element representation is the fact that different sizes of elements can be employed in different parts of the system during a single analysis. Thus, it is possible to employ small elements in regions of stress concentration and high

stress gradients, while larger elements may be used in areas where the stresses are relatively constant.

The principal disadvantage of the finite element method also results directly from the discrete nature of the idealization. Because the stresses are assumed constant within each element, the discontinuous stress distribution which is computed must be smoothed out graphically to give a better indication of the actual continuous distribution. In the construction of the stress contours in this study, it was assumed that the calculated element stress applied to the center of the element, and the contour lines were located accordingly. Increasing the number of elements tends to reduce the stress discontinuities, of course, but because the computation time increases rapidly with the number of elements, it is desirable to do a certain amount of smoothing graphically.

ACKNOWLEDGMENT

Work described in this report was carried out under a University of California, Institute of Engineering Research Contract for the Little Rock District, U. S. Army Corps of Engineers. The authors particularly wish to thank Mr. E. F. Rutt, Chief of the Engineering Division of the Little Rock District, and the Board of Consultants to the District: Dr. R. W. Carlson, Professor R. E. Davis, and Mr. B. W. Steele, for their advice during the course of the investigation.

In addition, Mr. Ian King, graduate student at the University of California, is thanked for the very great part he played in the digital computer analyses. The support of the National Science Foundation, whose research grant made possible the original development of the computer program used in these analyses, is also gratefully acknowledged.

REFERENCES

[1] CLOUGH, R. W. — "The Finite Element Method in Plane Stress Analysis", *Proceedings*, Second Conference on Electronic Computation, ASCE Structural Division, Pittsburgh, Pennsylvania, September 1960, p. 345.

[2] CLOUGH, R. W. — "The Stress Distribution of Norfork Dam", University of California, *Institute of Engineering Research Report*, Series 100, Issue No. 19, March 1962.

[3] LEHMANN, F. G. — "Simultaneous Equations Solved by Over-Relaxation", *Proceedings*, Second Conference on Electronic Computation, ASCE Structural Division, Pittsburgh, Pennsylvania, September 1960, p. 503.